PHYSICAL REVIEW E **81**, 020903(R) (2010)

Experimental evidence of strong anomalous diffusion in living cells

Naama Gal and Daphne Weihs*
Faculty of Biomedical Engineering, Technion–Israel Institute of Technology, Haifa 32000, Israel
(Received 30 June 2009; revised manuscript received 1 December 2009; published 11 February 2010)

We evaluated the transport of polymeric particles internalized into living cancer cells. The mean-square displacement demonstrates superdiffusion with a scaling exponent of 1.25. Scaling exponents of a range of displacement moments are bilinear with moment order, exhibiting slopes of 0.6 and 0.8. Thus, we present experimental evidence of strong anomalous diffusion. Bilinearity indicates that particle motion is composed of subdiffusive regimes separated by active yet nonballistic flights. We discuss the results in terms of particle interactions with their microenvironment.

DOI: 10.1103/PhysRevE.81.020903 PACS number(s): 87.16.Uv, 05.40.Jc, 47.63.mh

Motion of particles embedded within living cells can provide an indication of the local intracellular structural-density and active transport processes. Recently, spontaneous motion of internalized [1–4] and endogenous particles [5–8] or externally driven particle motion [9,10] have been used to evaluate intracellular mechanics. The dynamics of particle motion are often characterized by the time-dependent mean-square displacement (MSD). The logarithmic slope of the time-dependent MSD, noted by an exponent α: $\langle|r(t+\tau)-r(t)|^2\rangle \sim \tau^{\alpha}$, provides an indication of the type of motion. For Brownian diffusion $\alpha=1$, whereas subdiffusion and superdiffusion correspond to $0\leq\alpha<1$ and $1<\alpha\leq 2$, respectively. However, the MSD and α cannot always reflect the existence of more than one simultaneous mode of motion. For example, active fluctuations of microtubule filaments in actin networks, driven by myosin motors, exhibit a diffusive-like motion or $\alpha=1$ [11]. Recently, simulations have shown that transient local trapping and escape by active convection gave rise to an MSD with a slope of ~ 1 [12]. Thus, in addition to the MSD, other measures are sometimes required to fully describe complex motion.

Expanding on the second moment, other moments of the displacement can further characterize particle transport. The time dependence of the qth moment of the displacement is hence defined by a scaling exponent $\lambda(q)$, where $\langle|r(t+\tau)-r(t)|^q\rangle \sim \tau^{\lambda(q)}$. Scale-invariant transport processes are characterized by scaling exponents $\lambda(q)$ that are linear with the moment order q. For example, in Brownian motion $\lambda(2)=\alpha=1$, and linearity entails $\lambda(q)=q/2$ for all q. Similarly, at the ballistic limit $\lambda(q)$ is linear with q value and has a slope of unity. Nonlinear $\lambda(q)$ of various forms have been demonstrated in several analytical and numerical works on complex transport systems such as chaotic systems [13,14], bounded or truncated Lévy flights [15–17], and multifractal random walks [18,19]. In the last decade, the term strong anomalous diffusion has been used to describe superdiffusive motion exhibiting nonlinear $\lambda(q)$; there, $\lambda(q)/q$ is a nondecreasing function of q [20]. A similar term, weakly self-similar diffusion, has been used to describe nonlinear $\lambda(q)$, albeit not restricted to superdiffusion [21]. Strong anomalous diffusion has been demonstrated in analytical and numerical works on chaotic maps [14,20], nontrivial flow fields [20–22], and Lévy walks [23]. In those cases, motion exhibited variations of "trap-escape," with local regimes of diffusive and confined motion, separated by ballistic "flights" or "jumps." Those two modes of motion give rise to a bilinear function of the scaling exponents $\lambda(q)$. Despite being commonly applied in analytical and numerical works, few experimental works have employed this analysis approach and no experimental evidence of strong anomalous diffusion has been presented. Linear $\lambda(q)$ has been shown in intracellular particle motion [24], and nonlinear convex $\lambda(q)$ has been observed in zooplankton swimming [25,26]. Here, we show experimental evidence of strong anomalous diffusion with a piecewise linear $\lambda(q)$ in the motion of particles within living cells.

Polymeric particles were embedded in living cells as probes for local dynamics. Fluorescent carboxyl-coated polystyrene probe-particles, 100 or 200 nm in diameter, were used as is or coated with poly-L-lysine-g-poly(ethylene-glycol) (PEG) [27] to reduce protein adsorption [28]. We have evaluated particle dynamics in human metastatic breast-cancer epithelial cells (MDA-MB-231, ATCC) grown in complete DMEM. Particles were internalized by natural uptake (i.e. endocytosis) and dispersed in the cytoplasm [Fig. 1(a)]. Particles mostly localized near the nucleus and thicker regions of the cytoplasm, and none entered the nucleus. To further explore particle encapsulation, membranes were live stained with Vybrant DiO before particle introduction [Fig. 1(b)]. Following particle internalization, cells were fixed and imaged with a spectral-imaging Zeiss LSM510 confocal system, using a x63/1.4 NA oil objective. Encapsulation of some, but not all, particles was apparent for all particle types. That is a result of the endocytosis process and features of the epithelial, cancer cell line. No correlation between vesicle size and encapsulated-particle size or surface chemistry was observed. Large vesicles containing more than one particle were identified and excluded in the analysis process. Particles included in the analysis were either unencapsulated or encapsulated in small vesicles.

Particle motion in cells was tracked at high magnification and in real time. Logarithmic-phase cells were plated in chambered coverglasses (Lab-Tek, Nunc) and placed within a microscope stage-mounted incubator, maintaining 37 °C, 5% CO_2, and high humidity. Imaging was done with an in-

*Author to whom correspondence should be addressed; daphnew@tx.technion.ac.il

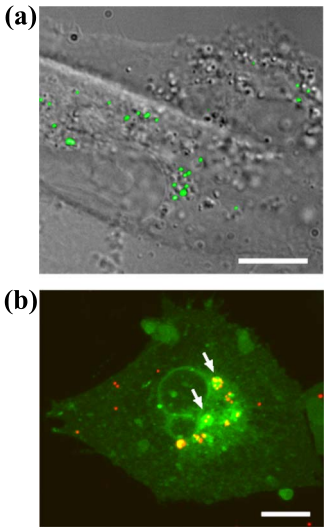

FIG. 1. (Color online) Human epithelial breast-cancer cells with internalized 200 nm particles. (a) Particles distributed within the cytoplasm of living cells. (b) Colocalization of live-stain membrane dye (green diffuse background) and internalized 200 nm carboxyl-coated particles (red, bright dots) indicates particle encapsulation in vesicles (arrows). Cells were fixed before imaging. Many particles but not all of them were encapsulated. Scale bars are 15 μm.

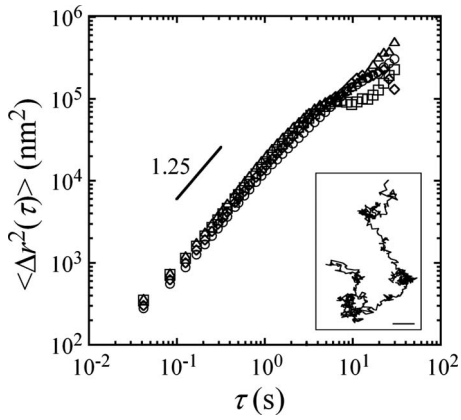

FIG. 2. Ensemble-averaged MSD of all particles in the cells. Markers are ◆ 100 nm carboxyl particles, ■ 100 nm PEG particles, ● 200 nm carboxyl particles, and ▲ 200 nm PEG particles. Line indicates logarithmic slope of 1.25. Inset: representative trajectory, demonstrating subballistic flights between local confined regimes. Scalebar: 50 nm.

verted, epifluorescence Olympus IX81 microscope, using a x100/1.4 NA DIC oil-immersion objective. Particle motion within cells was recorded at 24 frames/s using an Infinity 3-1M charge coupled device (CCD) camera (Lumenera) at a final magnification of 64.5-nm/pixel. No external forces were applied to the particles and cells and thus motion was driven by a combination of thermal fluctuations and natural active processes in the cells. For each particle type, 20–30 cells and over 200 particles were averaged. Frame-by-frame analysis of particle motion was done in MATLAB 2007b (Mathworks Inc.), using specialized algorithms that provide subpixel resolution of the time-dependent particle locations [4]; those are partially based on previously suggested algorithms [29]. Particle trajectories provided the time-dependent MSD for single particles as well as the ensemble.

The logarithmic slope of the MSD plot, α or $\lambda(2)$, provided an initial indication of particle dynamics within the cells. Ensemble averaged particle motion exhibited logarithmic slopes of $\alpha=1.25\pm0.01$, up to lag times of ~3 s, indicative of active transport in the cells (Fig. 2). Particle motion in controls of glycerol-water mixtures demonstrated $\alpha\sim1$. Moreover, following adenosine triphosphate (ATP) depletion, active transport in cells was reduced, and $\alpha\sim1$ was observed. Both those controls indicate that the superdiffusion observed in the untreated cells is likely driven by active cellular transport. Particle speeds at short lag times, as calculated between successive frames, were ~360 nm/s on average, within the range of molecular motor mediated motion at those time scales [30]. Active motion of internalized particles has been well established and several examples exist; that motion is associated with either direct coupling to motor proteins [2] or with nonthermal fluctuations of the cytoskeletal network [6,31]. Several parameters affect the value of α, among them are structure and density of the intracellular matrix, lag time, and particles size and surface chemistry. The MSD scaling exponent of 1.25 obtained here is similar to that previously reported in 100–200 nm endosomes in the human malignant epithelial HeLa cells [32]. Slopes of ~1.5 were reported in a number of cell types from animal source [2,5,6,31]. Naturally, the observed MSD and its logarithmic slope depend on specifics of cell structure and type, where, for example, in stiff yeast cells $\alpha\sim0.75$ has been observed over a wide lag-time range [33]. In a recent work on *Dictyostelium* cells, an exponent of ~1.4 was found for a range of particle sizes [10]. However, in mammalian cells, smaller particles reduced the MSD scaling exponent [34]. Particles larger than a characteristic pore size become entrapped by the network, thus their motion requires an active force; smaller particles, which are not completely entrapped, can diffuse within the mesh in addition to the active transport. The MSD observed here is in line with previous literature, however the main result of this Rapid Communication is found in different displacement moments.

Moments of the ensemble-averaged two-dimensional displacements were plotted for various moment orders q. For each q value, the logarithmic slope of the lag-time dependent qth moment provided a scaling exponent $\lambda(q)$. Figure 3 shows the scaling exponents, $\lambda(q)$, as a function of the moment order q. Fit ranges began at the minimal rate of 1/24 s and extended at least one logarithmic time decade; upper lag-time limit for each particle type was determined by the higher moment orders, where data became noisier. For all particle sizes and surface chemistries, scaling exponents exhibited a piecewise-linear function of q [Fig. 3(a)]. The observed functional form was

$$\lambda(q)=\begin{cases} A_1 q & q\le q_c \\ A_2 q - B_2 & q > q_c. \end{cases}$$

Fit parameters are presented in Table I. Motion of all particle types fit that nondecreasing nonlinear form and displayed $\lambda(2)>1$, satisfying the conditions for strong anomalous dif-

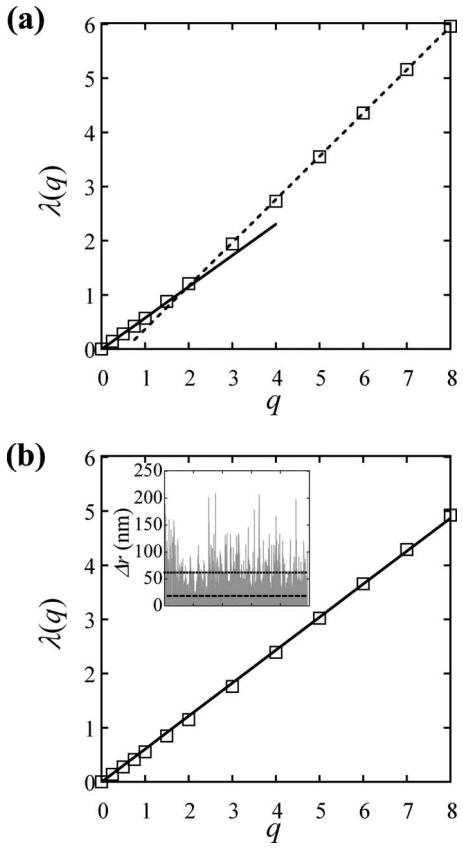

FIG. 3. Scaling exponents of displacement moments, $\lambda(q)$, as a function of the moment order q. Data presented are for 200 nm carboxyl-coated particles, representative of other particles. (a) Scaling exponents obtained from all displacements at short lag times. Fit lines are $\lambda(q)=0.58q$ at low q values and $\lambda(q)=0.8q-0.43$ at high q values. Error bars are on the order of the markers and were omitted for clarity. (b) Only displacements below the 3σ cutoff are considered. When large displacements were excluded, $\lambda(q)$ was linear with moment order q. Slope is 0.62, similar to the slope obtained at low q values without exclusion. Inset: Displacements Δr at lag-time 0.0833 s. Dashed line is at three standard deviations from the mean, $3\sigma=62$ nm, typical displacements are below that value.

fusion [20]. At low moment orders, up to a critical value of $q_c=1.5$, slopes of the scaling exponents were ~0.58 for all particle types and fits passed through the origin (Table I). Thus, at those moments a single exponent fully characterizes the anomalous transport process, as indicated by the constant $\lambda(q)/q$. The slopes $\lambda(q)/q$ observed here are qualitatively and quantitatively similar to simulations in physical systems [20–22]. At higher moment orders, $\lambda(q)$ of the different particles varied from 0.73 to 0.84 (Table I); here fits did not pass through the origin, and $\lambda(q)/q$ was not constant. Slopes and intercepts of $\lambda(q)$ at higher moment orders were particle-type dependent. Larger particles and biologically inert PEG-coated particles resulted in higher slopes, indicating more active transport.

We have validated that the piecewise-linear form of the scaling exponents results from rare active transport events in the cells. Occasional large displacements outstand from the common smaller ones as demonstrated in the inset of Fig. 3(b). Larger displacements were excluded using a cutoff of three standard deviations away from the mean; those amounted to less than 2% of the trajectory steps for all particle types. The scaling exponents of the remaining data [Fig. 3(b)] became linear with all q values. The single slope obtained following data filtration was ~0.62, similar to the slopes obtained at low q values when all displacements were considered (Table I). The induced linearity of the scaling exponents indicates that those large excluded steps were responsible for the nonlinearity and originate from active processes. That of course does not imply that the remaining displacements, which are still superdiffusive, result from a single transport mechanism.

The bilinearity of the scaling exponents suggests that particles experience local regimes of Brownian or confined motion separated by flights or jumps of enhanced diffusion [13,19–22]. Those events can, for example, be caused by occasional dragging by motor proteins of from intermittent collisions with (actively transported) adjacent vesicles and organelles. Recently, a temporal analysis approach was introduced, which identifies transient active phases in particle transport, where the MSD scaling exponent is close to 2 and the angle correlation function is close to zero, indicating directionality [1]. When applying that analysis approach to our data, only few particles exhibited any so-defined independent active regimes. Hence, the flights here are not strictly ballistic and directional but rather subballistic with a significant underlying diffusive or subdiffusive component. Indeed, that type of motion is often observed in our trajectories as demonstrated by the inset of Fig. 2. In addition, the subballistic flights lead to the ~0.8 slope of the scaling exponents at high moment orders, where in theoretical works, flights were ballistic, and scaling exponents had a slope of 1 at high q val-

TABLE I. Fits of scaling exponent, $\lambda(q)$, for different particle types.

	Fits of all displacements		Fits of displacements below 3σ cutoff
Probe particle	$0\le q\le 1.5$ [a]	$2\le q\le 8$ [a]	$0\le q\le 8$ [a]
200 nm PEG	$(0.60\pm0.01)q$	$(0.84\pm0.006)q$-(0.44 ± 0.02)	$(0.65\pm0.01)q$
200 nm carboxyl	$(0.58\pm0.009)q$	$(0.80\pm0.007)q$-(0.43 ± 0.03)	$(0.61\pm0.01)q$
100 nm PEG	$(0.56\pm0.01)q$	$(0.79\pm0.01)q$-(0.33 ± 0.05)	$(0.60\pm0.01)q$
100 nm carboxyl	$(0.57\pm0.01)q$	$(0.73\pm0.006)q$-(0.24 ± 0.007)	$(0.62\pm0.01)q$

[a]Errors presented are standard errors obtained from linear fits of $\lambda(q)$ vs q, considering errors propagated from fits of each moment vs. lag time. The R^2 was at least 0.998 in every fit presented in the table.

ues. Here, flights are superdiffusive yet not ballistic.

We suggest that the subballistic nature of flights results from the small particle size used in this work. As discussed above, smaller particles can diffuse more freely within the dense cytoplasm as compared to larger ones [34]. That is in agreement with the MSD scaling exponent, which is lower than was reported for micron sized particles. Thus, active flights of the smaller particles are more wiggly and less ballistic. Correspondingly, our results show that the slope of the scaling exponents at high moment orders is larger (i.e. closer to 1) for 200 nm particles as compared to 100 nm ones (Table I). Similarly, for a given particle size, PEG coating reduces protein adsorption and enhances particle motion [28,35], making those flights closer to ballistic with larger slopes at higher moment orders (Table I). Thus, the slope of the scaling exponents can provide information on the coupling between the particle and the intracellular matrix.

To conclude, we have shown that submicron particles embedded within living cancer cells exhibit superdiffusion with $\alpha \sim 1.25$. Enhanced diffusion of those particles gives rise to strong anomalous diffusion. Scaling exponents of the displacement moments, $\lambda(q)$, exhibit a piecewise linear dependence on the moment order, q. The bilinearity of scaling exponents suggests that particle motion is composed of local regimes of Brownian and confined motion separated by active flights. When rare large displacements were excluded from analysis, scaling exponents became linear with q, and strong anomalous diffusion was no longer observed. However, slopes of ~ 0.8 (and not 1) at high moment orders, together with lack of directionality, indicate that flights are not purely ballistic but rather have a significant diffusive component. We suggest that the subballistic flights are due to small particle size and that slopes of scaling exponents can be related to the interaction of the particle with the intracellular network. Hence, we have shown that higher moments of the displacement can provide increased understanding of particle motion in active systems. This approach can be used to augment analysis of transport in live cells, as well as in many complex fluid dynamics systems.

The authors thank Professor Alexander Nepomnyashchy and Professor Dov Levine for their valuable suggestions and stimulating discussions. Partially supported by the Israeli Ministry of Health, the Israeli Ministry of Science, and the Technion VPR fund.

[1] D. Arcizet *et al.*, Phys. Rev. Lett. **101**, 248103 (2008).
[2] A. Caspi, R. Granek, and M. Elbaum, Phys. Rev. Lett. **85**, 5655 (2000).
[3] D. Weihs, T. G. Mason, and M. A. Teitell, Biophys. J. **91**, 4296 (2006).
[4] D. Weihs, T. G. Mason, and M. A. Teitell, Phys. Fluids **19**, 103102 (2007).
[5] B. D. Hoffman *et al.*, Proc. Natl. Acad. Sci. U.S.A. **103**, 10259 (2006).
[6] A. W. C. Lau *et al.*, Phys. Rev. Lett. **91**, 198101 (2003).
[7] S. S. Rogers, T. A. Waigh, and J. R. Lu, Biophys. J. **94**, 3313 (2008).
[8] S. Yamada, D. Wirtz, and S. C. Kuo, Biophys. J. **78**, 1736 (2000).
[9] A. H. B. de Vries *et al.*, Biophys. J. **88**, 2137 (2005).
[10] C. Wilhelm, Phys. Rev. Lett. **101**, 028101 (2008).
[11] C. P. Brangwynne *et al.*, Phys. Rev. Lett. **100**, 118104 (2008).
[12] D. Weihs, M. A. Teitell, and T. G. Mason, Microfluid. Nanofluid. **3**, 227 (2007).
[13] B. A. Carreras, V. E. Lynch, D. E. Newman, and G. M. Zaslavsky, Phys. Rev. E **60**, 4770 (1999).
[14] A. S. Pikovsky, Phys. Rev. A **43**, 3146 (1991).
[15] I. Gleria *et al.*, Physica A **342**, 200 (2004).
[16] S. Painter and G. Mahinthakumar, Adv. Water Resour. **23**, 49 (1999).
[17] G. Terdik, W. A. Woyczynski, and A. Piryatinska, Phys. Lett. A **348**, 94 (2006).
[18] E. Bacry, J. Delour, and J. F. Muzy, Phys. Rev. E **64**, 026103 (2001).
[19] A. I. Saichev and V. A. Filimonov, J. Exp. Theor. Phys. **107**, 324 (2008).
[20] P. Castiglione *et al.*, Physica D **134**, 75 (1999).
[21] R. Ferrari, A. J. Manfroi, and W. R. Young, Physica D **154**, 111 (2001).
[22] X. Leoncini, L. Kuznetsov, and G. M. Zaslavsky, Chaos, Solitons Fractals **19**, 259 (2004).
[23] K. H. Andersen *et al.*, Eur. Phys. J. B **18**, 447 (2000).
[24] H. Ewers *et al.*, Proc. Natl. Acad. Sci. U.S.A. **102**, 15110 (2005).
[25] L. Seuront *et al.*, Zool. Stud. **43**, 498 (2004).
[26] F. G. Schmitt and L. Seuront, Physica A **301**, 375 (2001).
[27] S. Faraasen *et al.*, Pharm. Res. **20**, 237 (2003).
[28] M. T. Valentine *et al.*, Biophys. J. **86**, 4004 (2004).
[29] J. C. Crocker and D. G. Grier, J. Colloid Interface Sci. **179**, 298 (1996).
[30] C. Kural *et al.*, Science **308**, 1469 (2005).
[31] I. M. Kulic *et al.*, Proc. Natl. Acad. Sci. U.S.A. **105**, 10011 (2008).
[32] R. P. Kulkarni *et al.*, Biophys. J. **90**, L42 (2006).
[33] I. M. Tolic-Norrelykke *et al.*, Phys. Rev. Lett. **93**, 078102 (2004).
[34] A. Caspi, R. Granek, and M. Elbaum, Phys. Rev. E **66**, 011916 (2002).
[35] J. Suh *et al.*, Int. J. Nanomedicine **2**, 735 (2007).